The Plant Cell, Vol. 21: 106–117, January 2009, www.plantcell.org © 2009 American Society of Plant Biologists

SHORT HYPOCOTYL UNDER BLUE1 Associates with *MINISEED3* and *HAIKU2* Promoters in Vivo to Regulate *Arabidopsis* Seed Development [W]

Yun Zhou,[a] Xiaojuan Zhang,[b] Xiaojun Kang,[a,1] Xiangyu Zhao,[b,1] Xiansheng Zhang,[b,2] and Min Ni[a,2]

[a] Department of Plant Biology, University of Minnesota, St. Paul, Minnesota 55108
[b] State Key Laboratory of Crop Biology, College of Life Sciences, Shandong Agricultural University, Taian, Shandong, 271018, P.R. China

Seed development in *Arabidopsis thaliana* undergoes an initial phase of endosperm proliferation followed by a second phase in which the embryo grows at the expense of the endosperm. As mature seed size is largely attained during the initial phase, seed size is coordinately determined by the growth of the maternal ovule, endosperm, and embryo. Here, we identify SHORT HYPOCOTYL UNDER BLUE1 (SHB1) as a positive regulator of *Arabidopsis* seed development that affects both cell size and cell number. *shb1-D*, a gain-of-function overexpression allele, increases seed size, and *shb1*, a loss-of-function allele, reduces seed size. *SHB1* is transmitted zygotically. The increase in *shb1-D* seed size is associated with endosperm cellurization, chalazal endosperm enlargement, and embryo development. SHB1 is required for the proper expression of two other genes that affect endosperm development, *MINISEED3* (*MINI3*) and *HAIKU2* (*IKU2*), a WRKY transcription factor gene and a leucine-rich repeat receptor kinase gene. SHB1 associates with both *MINI3* and *IKU2* promoters in vivo. SHB1 may act with other proteins that bind to *MINI3* and *IKU2* promoters to promote a large seed cavity and endosperm growth in the early phase of seed development. In the second phase, SHB1 enhances embryo cell proliferation and expansion through a yet unknown IKU2-independent pathway.

INTRODUCTION

In angiosperms, double fertilization leads to the formation of a diploid embryo and a triploid endosperm, as the endosperm arises from the central cell that contains two identical haploid genomes. The endosperm constitutes the major volume of the mature seed in monocots and some dicots. In *Arabidopsis thaliana* and many other dicots, seed development is marked by two distinct phases (Sundaresan, 2005). In an initial phase, rapid growth and proliferation of the endosperm results in a large increase in size (Boisnard-Lorig et al., 2001). Then, embryo growth takes place at the expense of endosperm during the second phase. At maturity, the seed contains only a single layer of endosperm cells, and the maternal integument ultimately becomes the seed coat (Scott et al., 1998; Garcia et al., 2003). Seed coat formation and endosperm growth precede embryo growth in *Arabidopsis*, and the seed reaches almost its final size before the enlargement of the embryo. Therefore, seed size is determined by the coordinated growth of the diploid embryo, the triploid endosperm, and the diploid maternal ovule.

Both maternal and nonmaternal factors are involved in seed size regulation (Garcia et al., 2005). In *Arabidopsis*, an increased dosage of the paternal genome in the endosperm increases seed size, whereas an increased dosage of the maternal genome reduces seed size, with delayed cellularization of the peripheral endosperm and hypertrophy of the chalazal endosperm and associated nodules (Scott et al., 1998). Mutations in *DNA METHYLTRANSFERASE1* (*MET1*) and *DECREASE IN DNA METHYLATION1* (*DDM1*) dramatically reduce DNA methylation and cause parent-of-origin effects on F1 seed size (Xiao et al., 2006). Pollination of *met1-6* or *ddm1-2* pistils with wild-type pollen produced larger F1 seeds with a hypomethylated maternal genome, delayed endosperm development, and a larger endosperm volume than the wild type. A reciprocal cross led to small F1 seeds with a hypomethylated paternal genome, early endosperm cellularization, and, ultimately, a smaller endosperm volume than the wild type.

The seeds of the triple cytokinin receptor mutant are twice the size of wild-type seeds, and cytokinin may regulate embryo size via a maternal and/or endospermal mechanism (Hutchison et al., 2006; Riefler et al., 2006). Mutations in the transcription factor *APETALA2* (*AP2*) increase seed size due to an increase in both embryonic cell number and cell size, and the seed trait is passed through the maternal sporophyte and the endosperm genomes (Jofuku et al., 2005; Ohto et al., 2005). The integument also plays a role in seed size determination, and the *Arabidopsis mega-integumenta/auxin response factor2* mutant causes extra cell division in the integuments surrounding the mutant ovules, enlarges seed coats, and increases seed size (Schruff et al., 2006).

[1] These authors contributed equally to this work.
[2] Address correspondence to nixxx008@tc.umn.edu and zhangxs@sdau.edu.cn.
The author responsible for distribution of materials integral to the findings presented in this article in accordance with the policy described in the Instructions for Authors (www.plantcell.org) is: Min Ni (nixxx008@tc.umn.edu).
[W] Online version contains Web-only data.
www.plantcell.org/cgi/doi/10.1105/tpc.108.064972

Mutations in either *HAIKU2* (*IKU2*) or *MINISEED3* (*MINI3*) reduce seed size, and the mutant seed phenotypes depend on the genotype of both the embryo and the endosperm (Luo et al., 2005). *MINI3* encodes a WRKY family transcription factor and is expressed in both the endosperm and the embryo. *IKU2* encodes a leucine-rich repeat (LRR) receptor kinase and is expressed in the endosperm but not in the embryo or elsewhere in the plant. Interestingly, *IKU2* expression is downregulated in *mini3*, and MINI3 may act upstream of IKU2. The reduced seed size of the *iku* mutants is closely associated with a reduced growth of endosperm, a premature cellularization of the endosperm, and a reduced proliferation of the embryo after the early torpedo stage (Garcia et al., 2003). AGAMOUS-like 62 (AGL62) is another regulator of endosperm cellularization, as the endosperm cellularizes prematurely in *agl62* seeds (Kang et al., 2008).

SHORT HYPOCOTYL UNDER BLUE1 (SHB1) was initially isolated from a gain-of-function mutant, *shb1-D* or *short hypocotyl under blue 1-Dominant*, with a long hypocotyl phenotype under red, far-red, and blue light (Kang and Ni, 2006). Its recessive T-DNA knockout allele, *shb1*, exhibits a short hypocotyl phenotype under blue light. In this study, we show that SHB1 also has specific functions in *Arabidopsis* seed development, regulating endosperm proliferation and the timing of endosperm cellularization. SHB1 associates with *MINI3* and *IKU2* promoters, as demonstrated by chromatin immunoprecipitation (ChIP) analysis, and SHB1 may be recruited by other transcription factors that specifically recognize *MINI3* and *IKU2* promoter sequences.

RESULTS

shb1-D Produces Significantly Enlarged Seeds, and *shb1* Notably Reduces Seed Size

We determined the average seed mass by weighing mature dry *Arabidopsis* seeds in batches of 100 for seed lots from independently propagated Wassilewskija (Ws), *shb1-D*, Columbia (Col), and *shb1* lines or independent transgenic lines that overexpress either green fluorescent protein (GFP) or full-length SHB1:GFP. *shb1-D* and the SHB1:GFP overexpression (SHB1 OE) plants had seeds that were 1.5- to 1.7-fold heavier per 100 seeds or per silique than the Ws wild type, whereas the *shb1* mutation reduced seed mass by 15% compared with the Col wild type ($P < 0.01$, two-tailed Student's *t* tests) (Figures 1A and 1B). By contrast, the number of seeds per silique and the number of siliques per plant were not changed for Ws and *shb1-D* (Figure 1C; see Supplemental Figure 1A online). We harvested all seeds from each plant, and, as shown in Figure 1D, the seed mass of *shb1-D* plants was increased compared with Ws wild type, and the seed mass of *shb1* was notably reduced compared with Col ($P < 0.001$, two-tailed Student's *t* tests).

Seed Enlargement of *shb1-D* Is Due to Increases in Cell Size and Cell Number

We isolated and visualized embryos from mature seeds and found that the cotyledon area of *shb1-D* was 1.5-fold larger than

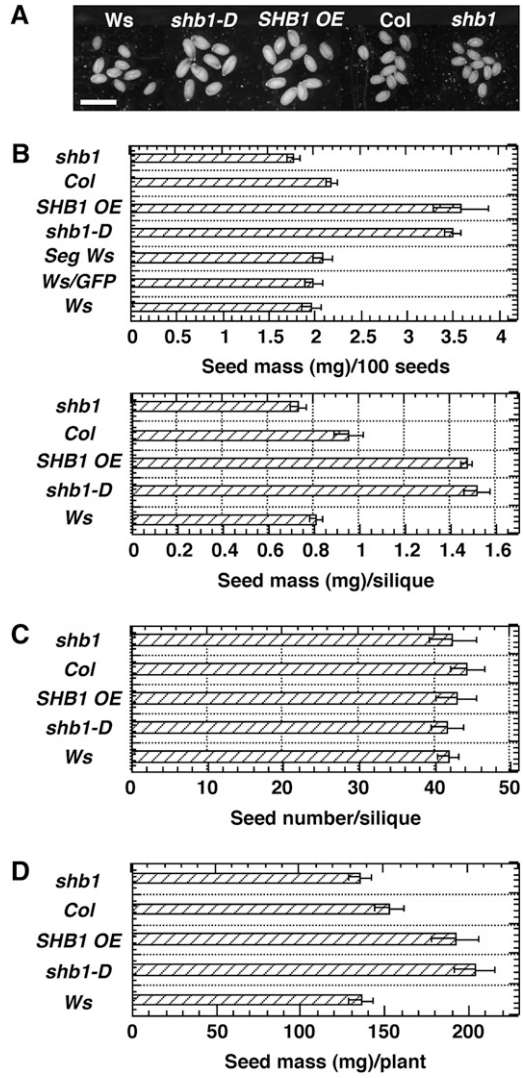

Figure 1. SHB1 Regulates Seed Size.

(A) Mature seeds of Ws, *shb1-D*, *SHB1 OE*, Col, and *shb1*. Bar = 0.5 mm.
(B) Average seed mass per 100 seeds (top) or per silique (bottom) for Ws, *shb1-D*, *SHB1 OE*, Col, and *shb1*. Data from Ws plants that segregated from the original *SHB1 OE* lines or Ws plants that carry a GFP transgene are also shown as controls.
(C) Seed number per silique for Ws, *shb1-D*, *SHB1 OE*, Col, and *shb1*.
(D) Total seed mass (mg) for Ws, *shb1-D*, *SHB1 OE*, Col, and *shb1*. Data are means ± SE from at least six independently propagated wild-type and mutant lines or independent transgenic lines.

that of the Ws wild type (Figures 2A and 2B). The embryonic shoot or hypocotyl and embryonic root apex of *shb1-D* also appeared larger than those of the Ws wild type (Figure 2A). We further examined whether the seed size increase of *shb1-D* is due to an increase in cell division or cell expansion. The average size of *shb1-D* cotyledon cells is 1.2-fold that of the wild type (Figure 2B). The size of *shb1-D* hypocotyl cells also appeared larger than that of the Ws wild type (Figure 2C). We then monitored the

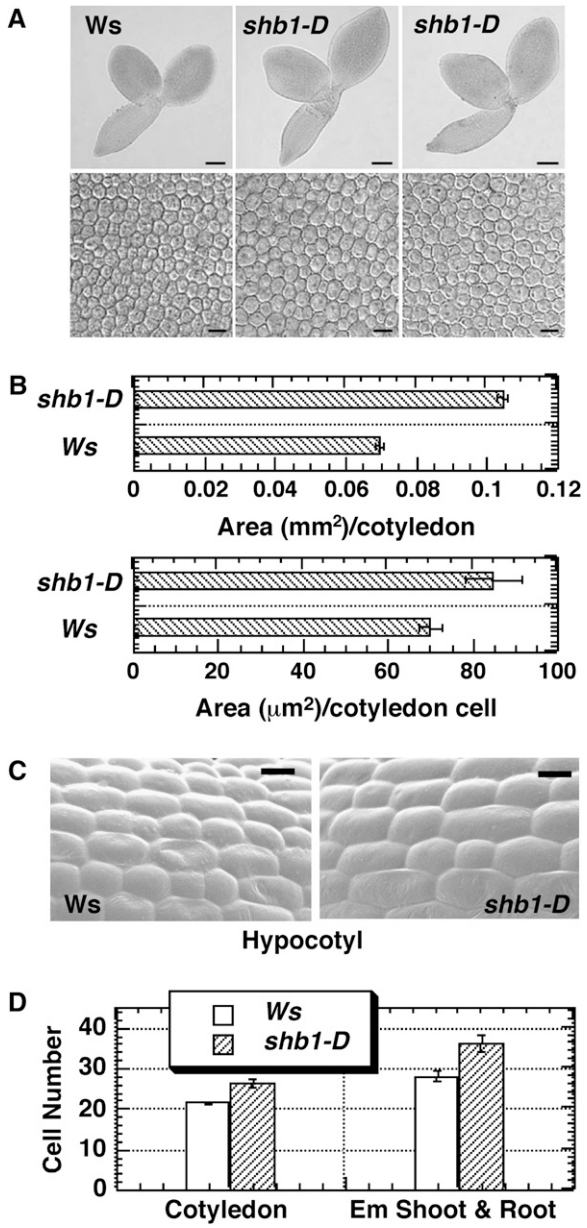

Figure 2. The Increase in Seed Size of *shb1-D* Is Due to an Increase in Both Cell Size and Cell Number.

(A) Mature embryos dissected from imbibed seeds of Ws (top left) and *shb1-D* (top right) plants. Epidermal cell layer from the central region of Ws (bottom left) and *shb1-D* (bottom right) cotyledons. Bars = 100 μm in top panels and 10 μm in bottom panels.

(B) Cotyledon area (top) and cotyledon cell size (bottom) of Ws and *shb1-D* plants.

(C) Epidermal cell layer from the central region of Ws (left) and *shb1-D* (right) hypocotyls. Bars = 50 μm.

(D) Average cell numbers from three columns in the central region of the cotyledon (left) and the hypocotyl plus the embryonic (Em) root (right) in Ws and *shb1-D* plants. Data in **(B)** and **(D)** are means ± SE from at least 20 independently propagated Ws or mutant lines.

numbers of epidermal cells in mature embryos under scanning electron microscopy and counted the cell number from three columns in the central region of cotyledons or in the hypocotyl plus the embryonic root of Ws and *shb1-D*. The average number of cells in the cotyledon and in the hypocotyl plus the embryonic root was 1.23- and 1.29-fold greater, respectively, in *shb1-D* than in the Ws wild type (Figure 2D). Interestingly, the 1.2-fold increase in cell size (Figure 2B) and 1.23- to 1.29-fold increase in cell number accounted for a 1.44- to 1.56-fold increase in embryo size of *shb1-D*. Therefore, both increased cell size and cell number contribute to the overall enlargement of mature embryo in the gain-of-function mutant *shb1-D*.

shb1-D Seeds Accumulate More Proteins and Fatty Acids Than Do Wild-Type Seeds

The differences in seed mass between *shb1-D* or *shb1* plants and wild-type plants may be due in part to an increase or a decrease in seed reserves, respectively. We prepared protein extracts from 200 seeds each of Ws wild type or *shb1-D* and examined the content and spectrum of soluble proteins. Two major classes of *Arabidopsis* seed storage proteins include the 12S cruciferins and the 2S albumins (Heath et al., 1986; Pang et al., 1988). The seeds of *shb1-D* or the SHB1 OE plants accumulated 1.5-fold more proteins, when expressed as mg/100 seeds, than those of the Ws wild type (Figure 3A). By contrast, the total protein content was reduced by >20% in *shb1* plants relative to the Col wild type ($P < 0.01$, two-tailed Student's *t* tests). No such difference in protein content was detected when expressed on the basis of seed weight, and the increase in protein content is apparently due to the larger seeds and not a higher concentration of protein in the seeds (see Supplemental Figure 3A online). The spectrum of the seed storage proteins or the relative proportion of 12S storage proteins to other proteins was not selectively affected by the *shb1-D* mutation, whereas the 2S albumin proteins were not retained in the 12% SDS-PAGE gel (Figure 3B). We also measured the content of reducing sugars and total soluble sugars in wild-type and *shb1-D* mutant seeds. *shb1-D* and SHB1 OE lines accumulated more reducing sugars and total soluble sugars per seed than did Ws, and the *shb1* mutant accumulated less sugars per seed than did Col (see Supplemental Figure 4 online).

We next measured the content and composition of total fatty acid methyl-ester for Ws wild-type and *shb1-D* mutant seeds. Like *Brassica napus*, *Arabidopsis* seeds contain a small number of fatty acid species that represent ~80% of the total fatty acid content in seeds (Downey 1983; James and Dooner, 1990; Taylor et al., 1995). As shown in Figure 3C, *shb1-D* accumulated more total fatty acids per seed due to increased seed size than did Ws, and a 20% reduction in total fatty acid content per seed was observed in *shb1* relative to Col ($P < 0.01$, two-tailed Student's *t* tests). By contrast, the fatty acid composition, including palmitic (C16:0), palmitoleic (C16: 1), stearic (C18:0), oleic (C18: 1), linoleic (C18: 2), linolenic (C18: 3), arachidic (C20:0), eicosenoic (C20: 1), behenic (C22:0), and erucic (C22:1) acids, was not significantly altered between *shb1-D* and Ws or *shb1* and Col plants (see Supplemental Figure 3B online).

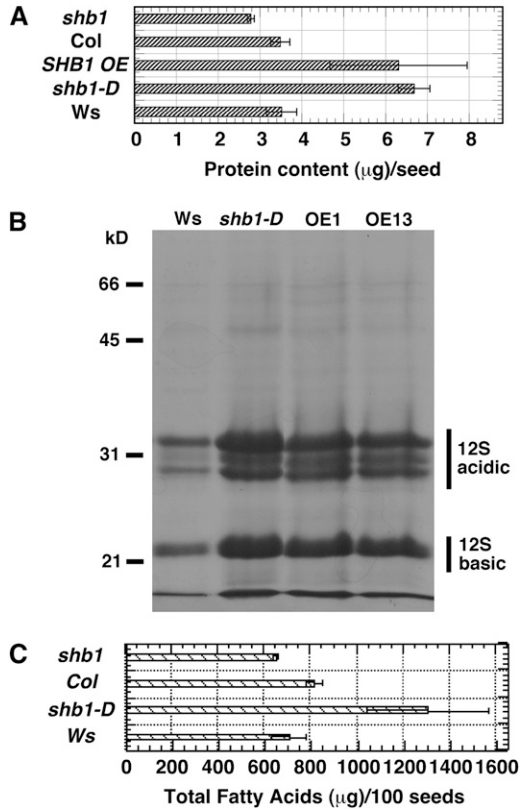

Figure 3. *shb1-D* Seeds Have Higher Protein and Fatty Acid Content Than Do Ws Seeds.

(A) Total protein content per seed for Ws, *shb1-D*, *SHB1 OE*, Col, and *shb1*.
(B) Spectrum of seed storage proteins in Ws, *shb1-D*, and *SHB1 OE*. Molecular standard ladder is shown to the left of the gel.
(C) Total fatty acid methyl-ester content per 100 seeds of Ws, *shb1-D*, Col, and *shb1*. Data are means ± SE from at least six independently propagated Ws, mutant lines, or independent transgenic lines.

Activation of *SHB1* Enlarges the Seed Cavity and Delays Endosperm Cellularization and Embryo Development

To explore the developmental alterations of *shb1* mutants, cleared seeds of *shb1-D* or *shb1*, and also of their corresponding wild types, were compared at different developmental days after pollination (DAP) (Figure 4). The embryo sac or seed cavity in the *shb1-D* mutant was significantly larger than that of the Ws wild type at 4 DAP and remained larger throughout embryogenesis. By contrast, *shb1-D* embryos were developmentally delayed compared with those of Ws at the early phase of seed development but gradually caught up at the later phase of seed development to obtain a larger size than those of the wild type at maturity (Figures 1 and 4). By contrast, the *shb1* embryo sac was similar in size or slightly smaller than that of Col from 4 to 9 DAP, and the embryo of *shb1* was smaller than that of Col at 9 DAP (Figure 4). Seeds of *shb1-D* were longer, wider, and more pointed at the micropylar pole than those of Col (Figure 5A). By 5 DAP, wild-type seeds had reached the late heart stage, the chalazal endosperm formed a compact rounded cyst, and the peripheral endosperm was cellularizing from the micropylar pole (Figures 4 and 5A). By contrast, *shb1-D* seeds of the same age had globular to early heart stage embryos and long and enlarged chalazal endosperms, and the peripheral endosperm had not undergone substantial cellulerization by this stage, as that seen in the Ws wild type (Figure 5A).

SHB1 Acts Zygotically to Regulate Seed Size

To determine the mode of transmission of parental *SHB1*, we performed reciprocal crosses between Ws and *shb1-D* or between Col and *shb1* using flowers at identical positions (11th to 14th flowers) on secondary inflorescences. Seed masses were determined from five inflorescences per plant and four to five

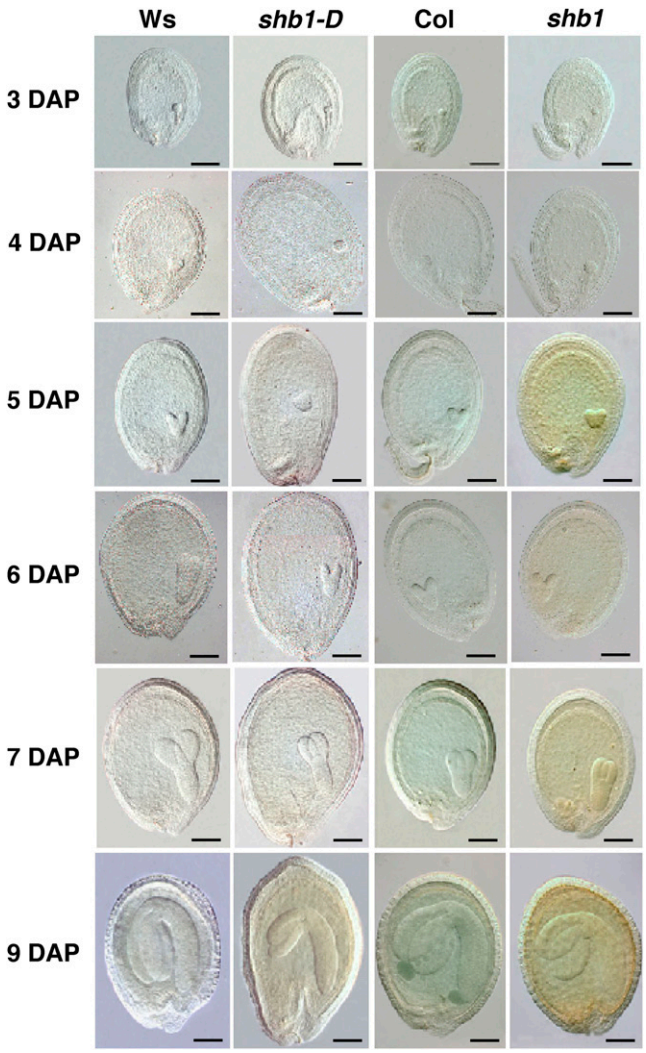

Figure 4. Seed Development in Wild-Type and *shb1* Mutant Plants.

Cleared Ws, *shb1-D*, Col, and *shb1* seeds were imaged with differential contrast optics at 3, 4, 5, 6, 7, and 9 DAP. Bars = 50 μm.

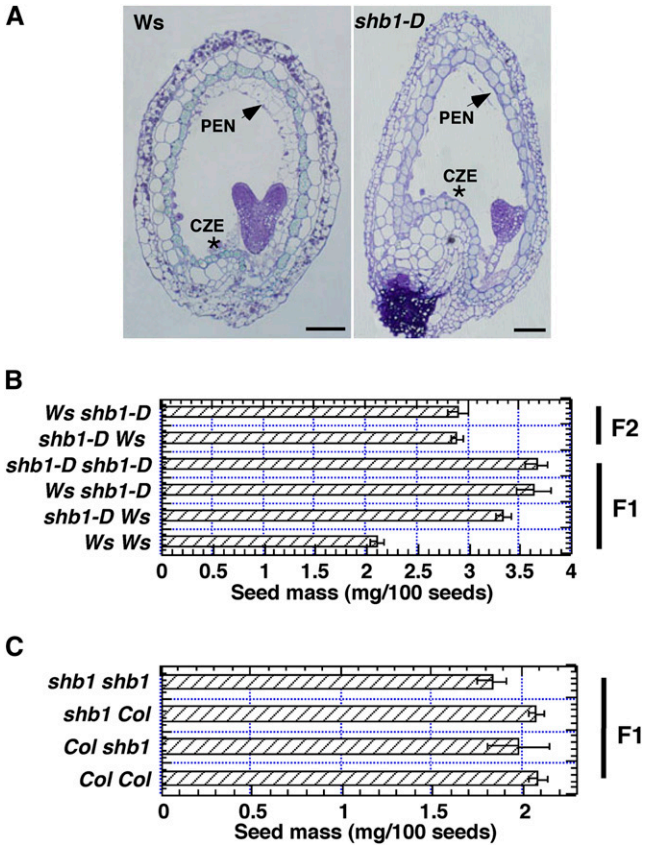

Figure 5. The *shb1-D* Mutation Affects Endosperm Development, and *SHB1* Is Transmitted Zygotically.

(A) Five-day-old Ws seed at the heart stage, with cellularized peripheral endosperm, and *shb1-D* seed at the late globular stage, with uncellularized endosperm. PEN (arrow), peripheral endosperm; CZE (asterisk), chalazal endosperm. Bars = 50 μm.

(B) F1 and F2 seed mass from reciprocal crosses between Ws and *shb1-D*. Ws *shb1-D* indicates Ws pollen crossed to a *shb1-D* pistil.

(C) F1 seed mass from reciprocal crosses between Col and *shb1*. Data are presented as means ± SE from at least six independently propagated Ws, Col, or mutant lines.

plants in total. If *SHB1* acted through the sporophyte genome to regulate seed mass, the effect of the dominant *shb1-D* mutation on seed mass would be observed only when maternal plants are homozygous or heterozygous in the *shb1-D* locus. As shown in Figure 5B, the dominant *shb1-D* allele regulates seed mass through the embryo genome in these reciprocal-cross experiments. The *shb1-D* (+/−) F1 seeds of *shb1-D* pistils pollinated with Ws wild-type pollen were heavier than wild-type seeds but were very close in weight to *shb1-D* (−/−) seeds produced when *shb1-D* pistils were pollinated with *shb1-D* pollen. The *shb1-D* (+/−) F1 seeds resulting from Ws wild-type pistils being pollinated with *shb1-D* pollen were also heavier than those of the wild type but were 12% lighter than *shb1-D* (−/−) seeds (Figure 5B). Apparently, maternal homozygous *shb1-D* mutants produced seeds that were consistently heavier than those from maternal wild-type plants due to a gene dosage effect from the triploid endosperm, and SHB1 may also partially act through the endosperm genome to regulate seed mass.

The large seed phenotype was still visible in a segregating F2 population for the two different reciprocal crosses performed. The F2 seeds from selfed *shb1-D* (+/−), regardless of maternal or paternal origin, all showed a 1.4-fold increase in seed mass compared with the Ws wild type (Figure 5B). The *shb1* (−/−) F1 seeds of *shb1* pistils pollinated with *shb1* pollen were, on average, 15% lighter than those of the Col wild type ($P < 0.01$, two-tailed Student's *t* tests) (Figure 5C). As *shb1* is recessive and has a relatively weak seed phenotype, *shb1* (+/−) F1 seeds formed in pistils either of *shb1* or of the Col wild-type produced seeds of the same mass as Col wild-type seeds (Figure 5C).

SHB1 Regulates the Expression of *MINI3* and *IKU2*

Through real-time RT-PCR analysis, we found that the *shb1-D* mutation enhanced, and the *shb1* mutation reduced, the expression of *MINI3* and *IKU2*, a WRKY family transcription factor gene and an LRR receptor kinase gene, but not that of *AP2*, a transcription factor gene involved in floral organ and seed development and expressed in the embryo but not in the endosperm ($P < 0.001$, two-tailed Student's *t* tests) (Figure 6A). The expression of *MINI3* in *shb1-D* green siliques was three times higher than in the Ws wild type, and the expression of *MINI3* in *shb1* was reduced by 40% compared with Col ($P < 0.001$, two-tailed Student's *t* tests) (Figure 6A). *IKU2* expression was 10-fold greater in *shb1-D* mutants and six-fold less in *shb1* mutants than in the Ws or Col wild type (Figure 6A). By contrast, the expression of *SHB1* relative to *UBQ10* in Col, *mini3*, *iku2*, and *ap2* was not changed (Figure 6B). In *shb1-D*, the expression of *IKU2* was enhanced by more than that of *MINI3*, and in the *shb1* mutant, the expression of *IKU2* was reduced by more than that of *MINI3*. *IKU2* is specifically expressed in the endosperm (Luo et al., 2005). To test if the altered expression of *IKU2* in *shb1-D* is caused by increased endosperm volume, we examined the expression of another endosperm-specific gene, *HEAT SHOCK FACTOR15* (*HSF15*) (Winter et al., 2007; http://bbc.botany.utoronto.ca/efp/cgi-bin/efpWeb.cgi) in the wild type and *shb1* mutants. No difference in *HSF15* expression was found between Ws and *shb1-D* or between Col and *shb1* (see Supplemental Figure 5A online).

SHB1 Acts Upstream of *MINI3* and *IKU2*

To test whether SHB1 acts upstream of *MINI3* and *IKU2*, we performed double mutant analysis, combining *shb1-D*, which produces large seeds, with either *mini3-2* (SALK_050364) or *iku2-4* (SALK_073260), which produce small seeds. As *shb1-D* (Ws) and *mini3-2* or *iku2-4* (Col) are in different genetic backgrounds, we performed the genetic analysis in a mixed Ws and Col background after a cross of *shb1-D* to either *mini3-2* or *iku2-4*. We selected the genotypes from the segregating F2 population by PCR genotyping, and at least 10 individuals of each genotype were identified and used in the analysis. As shown in Figure 6C, a mutation in *IKU2* diminished the large seed phenotype of *shb1-D*. Since the *shb1-D iku2-4* double mutant phenotypically resembled *iku2-4*, IKU2 appears to act downstream of

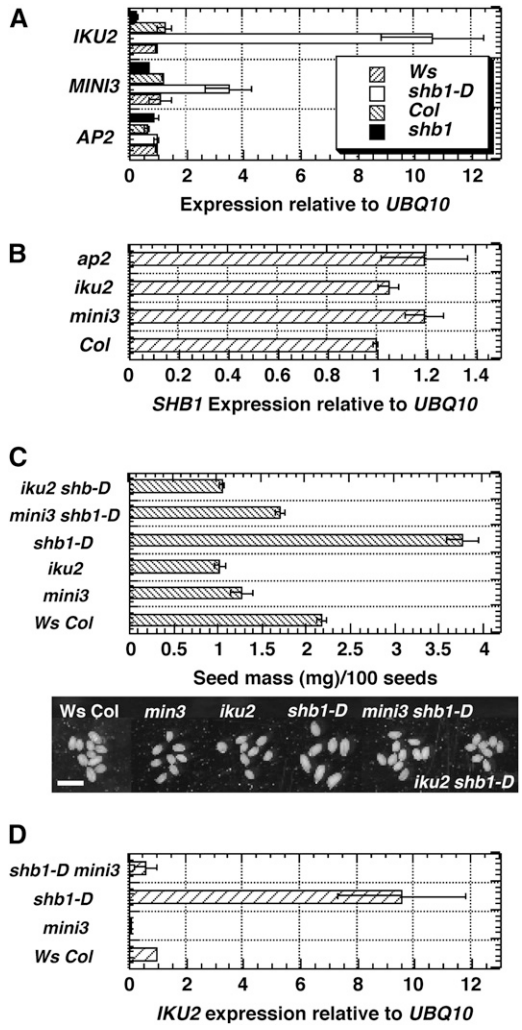

Figure 6. SHB1 Regulates the Expression of *MINI3* and *IKU2*.

(A) Expression of *MINI3*, *IKU2*, and *AP2* in Ws, *shb1-D*, Col, and *shb1* as determined by real-time RT-PCR analysis.

(B) Expression of *SHB1* in Col, *mini3* (*mini3-2*), *iku2* (*iku2-4*), and *ap2* as determined by real-time RT-PCR analysis.

(C) Genetic interactions of *SHB1* with *MINI3* and *IKU2*. All genotypes are in a mixed Ws/Col background identified from a F2 segregation population, and at least eight individuals were included in data calculation. Bar = 0.5 mm

(D) Expression of *IKU2* in Ws Col, *mini3*, *shb1-D*, and *shb1-D mini3* as determined by real-time RT-PCR analysis. Means were calculated from three biological samples, and each biological sample was examined in triplicate. The calculated SE includes technical error and biological error.

SHB1. The *mini3-2* mutation also significantly suppressed the large seed phenotype of *shb1-D* to that of the *mini3-2* single mutant (Figure 6C). We then examined the expression of *IKU2* in the *shb1-D mini3-2* double mutant. The mutation in *MINI3* completely blocked the expression of *IKU2* and reduced the expression of *IKU2* from a relative level of 10, as seen in the *shb1-D* single mutant, to a relative level of 0.6 (Figure 6D).

SHB1 Has an Overlapping Expression Pattern with *MINI3* and *IKU2*

To explore SHB1 function, we examined the expression pattern of a β-glucuronidase (GUS) reporter gene driven by a native *SHB1* promoter. GUS activity was observed in the apical meristem of young seedlings, rosette leaves, inflorescence, floral organs, mature pollen grains, germinating pollens, and mature unfertilized ovules (Figures 7A to 7F). The expression of *SHB1* overlaps with that of *MINI3* in floral buds, pollen grains, pollen tubes, and ovules (Figure 7; Luo et al., 2005). The expression of *SHB1* in developing seeds was also monitored by in situ hybridization. Within the developing siliques, *SHB1* has an overlapping expression pattern with *MINI3* in developing and cellularized endosperm and in the globular and early heart stage embryo 12 to 96 h after fertilization (Figures 7G to 7K; Luo et al., 2005). *SHB1* also has an overlapping expression pattern with *IKU2* in endosperm, and the expression of *IKU2* was only detected in the endosperm, but not in the embryo or elsewhere in the plant (Luo et al., 2005). In addition, *SHB1* expression was also detected in the chalazal endosperm or posterior cyst and in the late heart-stage and torpedo-stage embryos, suggesting a role for SHB1 in promoting embryonic development in the second phase of seed development (Figures 7G to 7J).

SHB1 Associates with *MINI3* and *IKU2* Promoters

To investigate how SHB1 regulates the expression of *MINI3* and *IKU2*, we performed a ChIP assay with either anti-SHB1 or anti-GFP antibodies followed by quantitative PCR analysis. Figure 8A shows the various amplicons in *MINI3* and *IKU2* promoters used for ChIP analyses. Amplicon M3, which spans from −986 to −1216 in the *MINI3* promoter, was highly enriched using either anti-SHB1 or anti-GFP antibodies, and amplicon M1, which spans from +3 to −349 in the *MINI3* promoter, was also significantly enriched (Figures 8B and 8C). By contrast, amplicon M2, which spans from −399 to −620 in the *MINI3* promoter, was not enriched (Figures 8B and 8C). Amplicon 1, which spans from −3 to −277 in the *IKU2* promoter, was moderately enriched, and amplicon 2, which spans from −296 to −665 in the *IKU2* promoter was significantly enriched (Figures 8B and 8C). We also performed ChIP analysis of the promoter sequences of *HSF15*, an endosperm-specific gene, and *LEAF COTYLEDON2* (*LEC2*; Stone et al., 2001), an embryo-specific gene, and neither of the promoter sequences was significantly enriched (see Supplemental Figures 5B and 5C online). In addition, SHB1 was unable to bind directly to either *MINI3* or *IKU2* promoter sequences in a gel mobility shift assay (Y. Zhou and M. Ni, unpublished data).

DISCUSSION

The Level of SHB1 Is Limiting during Seed Development

SHB1 has a specific function in endosperm and embryo development, as the sizes of many other organs, such as leaves, stems, roots, carpel, petals, and sepals, were not affected by either the *shb1-D* or the *shb1* mutation. SHB1 does not influence

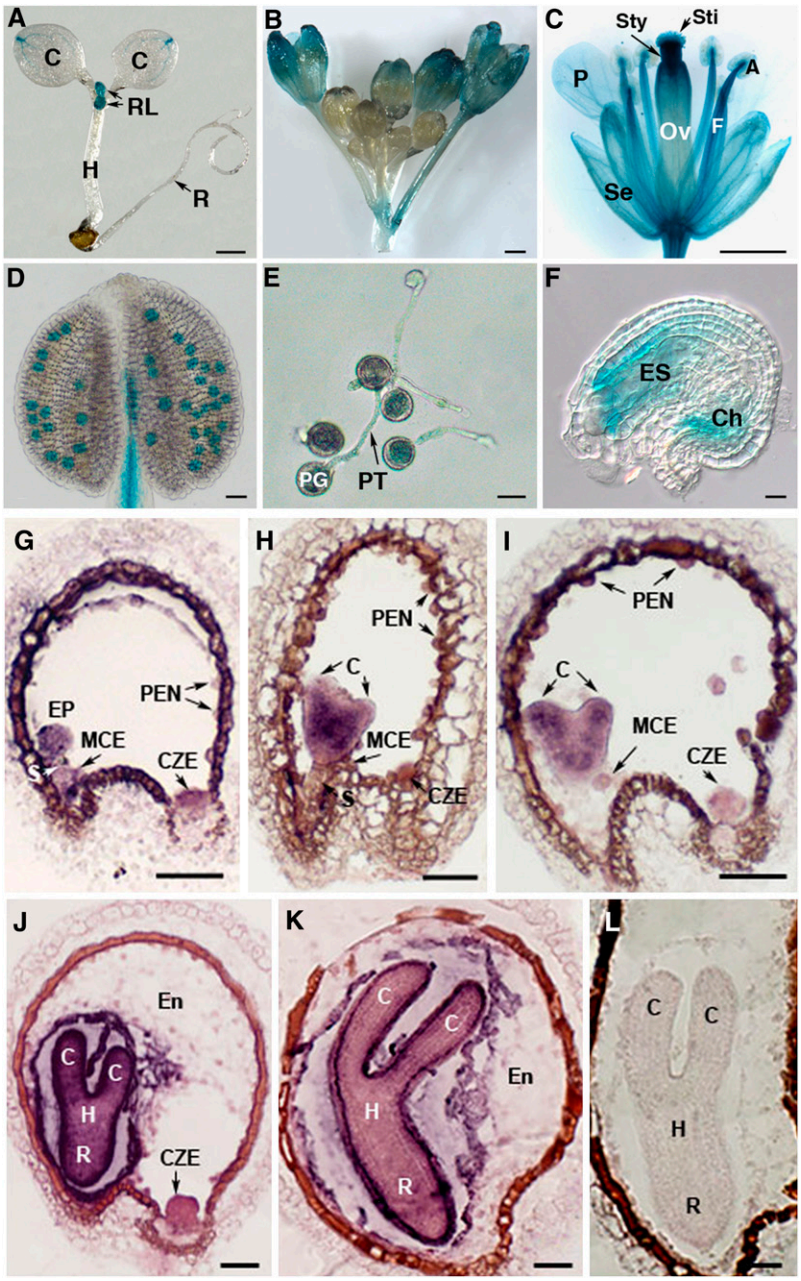

Figure 7. *SHB1* Is Expressed in Endosperm and Embryo.

Expression of *ProSHB1:GUS* in eight-day old seedling **(A)**, inflorescence **(B)**, flower **(C)**, mature pollen **(D)**, in vitro germinating pollen **(E)**, and unfertilized ovule **(F)**. In situ hybridization of Ws with *SHB1* antisense probe at early globular stage **(G)**, early heart stage **(H)**, heart stage **(I)**, torpedo stage **(J)**, and late torpedo stage **(K)** or with *SHB1* sense probe at torpedo stage **(L)**. A, anther; C, cotyledon; Ch, chalazal end; CZE, chalazal endosperm; En, endosperm; EP, embryo proper; ES, embryo sac; F, filament; H, hypocotyl; MCE, micropylar endosperm; Ov, ovule; P, petal; PEN, peripheral endosperm; PG, pollen grain; PT, pollen tube; R, embryonic root; RL, rosette leaf; S, suspensor; Se, sepal; Sti, stigma; Sty, style. Bars = 1 mm for **(A)** to **(C)**, 25 μm for **(D)** to **(F)**, and 50 μm for **(G)** to **(L)**.

general plant growth and development, and mature *shb1-D* or *shb1* plants were indistinguishable from those of the Ws or Col wild type (see Supplemental Figures 2A and 2B online). The seed phenotype is not tightly related to its function in light signaling since there was no particular enhancement of *shb1-D* or *shb1* seed size by red, far-red enriched, or blue light compared with white light (see Supplemental Figure 1B online). Although *SHB1* gain- or loss-of-function of mutants had altered seed size, *shb1* had a relatively weak phenotype, with a 15% reduction in seed mass, compared with a 1.5- to 1.6-fold increase in seed mass of

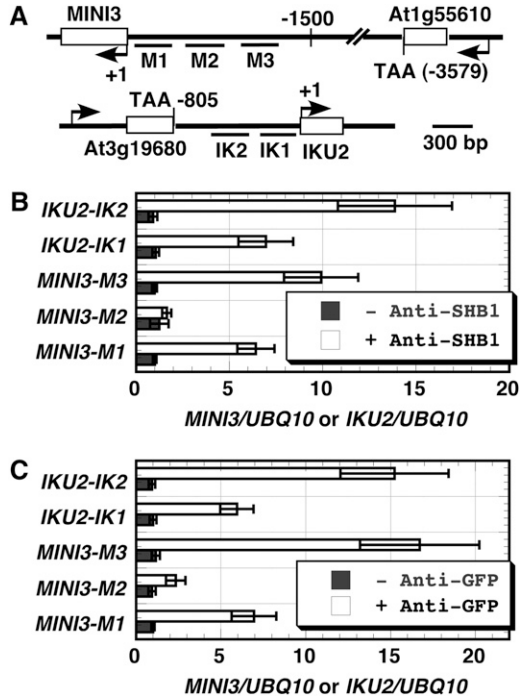

Figure 8. SHB1 Associates with *MINI3* and *IKU2* Promoters in Vivo.

(A) Schematic diagram of the *MINI3* and *IKU2* loci and the five amplicons (i.e., M1, M2, M3, IK1, and IK2) used for ChIP analysis.
(B) and **(C)** Enrichment of particular *MINI3* and *IKU2* chromatin regions with anti-SHB1 antibody in wild-type plants **(B)** or with anti-GFP antibody in SHB1:GFP transgenic plants **(C)** as detected by real-time PCR analysis. Preimmune serum was used as mock control. Means were calculated from three biological samples, and each biological sample was examined with three PCR technical replicates. The calculated SE includes technical error and biological error.

the *shb1-D* lines (Figure 1). The changes in protein or fatty acid content were also less dramatic in *shb1* than in *shb1-D* (Figure 3). The development of embryo sac and endosperm was not affected by the *shb1* mutation, but the embryo of *shb1* appeared smaller at 9 DAP than that of the wild type (Figure 4). One possibility is that the level of SHB1 is limiting for endosperm and seed enlargement since we were unable to detect *SHB1* message in regular RNA gel blot of total RNA prepared from rosette leaves, which show a strong SHB1 expression compared with other organ types by GUS reporter assay (Kang and Ni, 2006; Figure 7A). Therefore, SHB1 activation has a stronger effect on seed development than does the loss of SHB1. By contrast, the weak seed phenotype in *shb1* may be due to redundant SHB1 homologs or developmental pathways that regulate seed size. For example, one of the SHB1 homologs, gi 3548806 or At2g03240, is expressed at the globular and heart stages of the *Arabidopsis* embryo and has detectable expression levels in developing siliques (Winter et al., 2007; http://bbc.botany.utoronto.ca/efp/cgi-bin/efpWeb.cgi). The expression pattern of another SHB1 homolog, gi 3548805 or At2g03250, is not available in the public domain and merits further studies.

SHB1 Promotes Endosperm Enlargement at the Early Phase of Seed Development

The early phase of endosperm development in most species is marked by cell proliferation and growth to generate a large multinucleate cell and is defined as the syncytial phase (Olsen, 2001; Berger, 2003). This syncytium is then partitioned into individual cells by a specific type of cytokinesis called cellularization. Cellularization is initiated in the micropylar pole and occurs after the eighth mitotic cycle in the peripheral endosperm (Garcia et al., 2003). Endosperm development is essential for providing nutrients to the developing embryo and for enforcing a space limitation (Brink and Cooper, 1947). As the initial endosperm enlargement affects the final seed size, the endosperm may initiate a signal to regulate the subsequent embryo development (Miller and Chourey, 1992; Hong et al., 1996). The *mini3* and *iku* mutations cause premature cellularization of the endosperm and reduce the proliferation of the cellularized endosperm (Garcia et al., 2003; Luo et al., 2005). IKU and MINI3 may regulate endosperm size through the timing of endosperm cellularization (Luo et al., 2005). We demonstrated in this study that SHB1 gain-of-function regulates a similar set of cellular responses to MINI3 and IKU2, such as endosperm proliferation and the timing of endosperm cellularization (Figure 5A). More significantly, the activation of SHB1 significantly enlarges the embryo sac at 4 DAP, and the endosperm remains larger throughout the subsequent stages of seed development (Figure 4).

The posterior pole of the endosperm does not undergo cellularization and contains a multinucleate pool of cytoplasm, chalazal endosperm, or cyst. The cyst is located above the placentochalazal area of the seed integument where vascular elements terminate and is of potential importance for transfer of maternal nutrients to the seed (Schultz and Jensen, 1971; Otegui et al., 2002). The overall size of the posterior pole in *iku* seeds is reduced relative to that of the wild type, and cellularization reaches the posterior pole in a few *iku* seeds, suggesting that *iku*

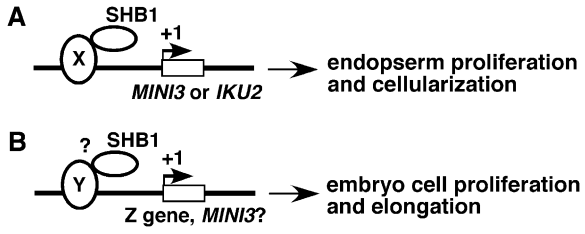

Figure 9. A Working Hypothesis Is Proposed for SHB1 Function in *Arabidopsis* Seed Development.

(A) SHB1 is recruited to the promoters of MINI3 and IKU2 by protein X and regulates the expression of key genes such as MINI3 and IKU2 that are required for endosperm proliferation and cellularization.
(B) It remains unknown if SHB1 deploys a similar mechanism to present itself through protein Y to the promoters of unknown targets such as Z gene or MINI3 that are essential for embryo cell proliferation and elongation. IKU2 is expressed uniquely in the endosperm, whereas MINI3 is expressed in both the endosperm and the embryo. MINI3 may play additional roles in embryonic development.

mutations cause a posterior displacement of the boundary between the peripheral endosperm and the posterior pole (Garcia et al., 2003). In the *shb1-D* mutant, the posterior cyst is significantly enlarged. This may result in an excess of nutrients from the maternal parent, which may contribute to the subsequent development of the embryo (Figure 5A).

SHB1 Regulates Embryo Cell Proliferation and Elongation at the Second Phase of Seed Development

The *mini3* and *iku* mutations also retard embryo proliferation after the early torpedo stage and reduce the total number of cells, but not the cell size, in the mature embryo (Garcia et al., 2003; Luo et al., 2005). Similarly, mutations in *EXTRA SPOROGENOUS CELLS*/*EXCESS MICROSPOROCYTES1* (*EXS*/*EMS*) also produced smaller seeds due to a reduction in cell size, but not in cell number (Canales et al., 2002; Zhao et al., 2002). *EXS*/*EMS* encodes a putative LRR receptor kinase and is expressed in both the embryo and the endosperm. The effect of the *iku2* mutation on embryo development may be indirect as a consequence of the effects of this mutation on the endosperm development at the initial phase of seed development. In addition, the expression of *IKU2* is limited to the endosperm (Luo et al., 2005). Although the endosperm may initiate a signal to regulate the subsequent embryo development, this hypothesis requires further validation. For example, it is still unknown if overexpression of *IKU2* promotes embryo development and leads to enlarged seeds. Although *MINI3* message can be detected in both the endosperm and embryo, it remains unknown if MINI3 functions in embryonic development in addition to its role in endosperm proliferation (Luo et al., 2005). By contrast, SHB1 activation causes active endosperm proliferation in the initial phase of seed development at the expense of embryonic development, but the embryo subsequently reaches its full mature size 2 to 3 d later than does the wild type. At maturity, the *shb1-D* mutation increases both embryo cell size and cell number (Figure 2). Therefore, SHB1 may activate other developmental pathways that regulate embryo cell division and cell expansion in addition to the MINI3-IKU2 pathway that regulates endosperm proliferation.

SHB1 Regulates the Expression of Both *MINI3* and *IKU2*

SHB1 is required for the proper expression of both *MINI3* and *IKU2* (Figure 6A). Double mutant analyses indicate that the effect of *shb1* mutations on seed development was largely dependent on MINI3 and IKU2 function (Figure 6C). SHB1 contains an N-terminal SPX (for SYG1, PHOSPHATE TRANSPORTER81, and XENOTROPIC AND POLYTROPIC MURINE LEUKEMIA VIRUSES RECEPTOR1) domain and a C-terminal EXS (for ER RETENSION-DEFECTIVE1, XENOTROPIC AND POLYTROPIC MURINE LEUKEMIA VIRUSES RECEPTOR1, and SYG1) domain (Kang and Ni, 2006). A major function of the SPX domain in yeast SYG1 protein is to mediate protein–protein interactions (Spain et al., 1995). The EXS domain contains several predicted transmembrane helices; however, SHB1 is localized to the nucleus (Kang and Ni, 2006). Thus, the EXS domain in SHB1 may have a distinct function from those in SYG1-like proteins. SHB1 protein does not contain DNA binding motifs that recognize specific elements in *MINI3* and *IKU2* promoters, and SHB1 did not directly bind to either the *MINI3* or *IKU2* promoter in a gel mobility shift assay (Y. Zhou and M. Ni, unpublished data). ChIP experiments indicate that SHB1 associates with *MINI3* and *IKU2* promoters in vivo (Figure 8). A similar function has been discovered for numerous other proteins, such as FLOWERING LOCUS T (FT), GIGANTEA (GI), and FLAVIN BINDING, KELCH REPEAT, F-BOX1 (FKF1) (Wigge et al., 2005; Sawa et al., 2007).

FT does not have DNA binding activity but associates with *AP1* promoters through a direct interaction with FLOWERING LOCUS D, a bZIP transcription factor that directly binds to the *AP1* promoter (Wigge et al., 2005). GI and FKF1 also associate with *CONSTANS* promoters through a direct interaction with CYCLING DOF FACTOR1, a Dof transcription factor, in a blue light–dependent manner (Sawa et al., 2007). Similarly, SHB1 may interact with other proteins that are specific transcription factors for *MINI3* and *IKU2* promoters and achieve its regulation over the transcription of *MINI3* and *IKU2* genes during the initial phase of seed development (Figure 9A). It remains unclear if SHB1 acts in a similar way to regulate embryo cell proliferation and elongation during the second phase of seed development (Figure 9B). Future studies will be directed to identify the protein factors that may interact with SHB1 in the regulation of either endosperm development or embryo development.

METHODS

Plant Materials and Growth Conditions

shb1 (SALK_128406), *mini3-2* (SALK_050364), *iku2-4* (SALK_073260), and *ap2* (SALK_071140) are in the Col background and were obtained from the ABRC (Ohio State University, Columbus). *shb1-D* was isolated in the Ws background, and the *SHB1* overexpression lines in the Ws or Col background were generated as described previously (Kang and Ni, 2006). *shb1-D* and *shb1* mutants were backcrossed twice to the wild type before phenotypic analysis. Plants were grown at 23°C, and all seeds from a single plant were harvested when the plant was mature and the last siliques on the inflorescence had elongated, turned brown, and dried. At the four-leaf stage, the younger plants were also fitted with a plastic well to catch all seeds released by dehiscing siliques in later developmental stages. These hand-harvested seeds were combined with those caught in the well, dried at 25°C for 7 d, and weighed.

Cytological Experiments

Mature seeds of Ws, *shb1-D*, *SHB1 OE*, Col, *shb1*, Ws/Col, *mini3-2*, *iku2-4*, *mini3-2 shb1-D*, and *iku2-4 shb1-D* were imaged with a Cool Cam color CCD camera (Cool Camera) coupled to a Nikon Eclipse E800 microscope, using Imago Pro Plus version 3.0 software (Media Cybernetics). Mature dried seeds of the wild type and *shb1* mutants were also imbibed for 1 h and dissected under a microscope to isolate mature embryos. The embryos was incubated for 12 h in buffer that contains 50 mM sodium phosphate, pH 7.0, 10 mM EDTA, 1% Triton X-100, and 1% DMSO at 37°C, fixed for 45 min in FAA (formalin, acetic acid, and ethanol) that contains 10% formalin, 5% acetic acid, 45% ethanol, and 0.01% Triton X-100, and dehydrated through an ethanol series (Ohto et al., 2005). The embryos were then treated for 1 h in Hoyer's solution that contains 3:0.8:0.4 of chloral hydrate:water:glycerol. Observations were made with a Zeiss 510 Meta confocal laser scanning microscope. Cotyledon area and average epidermal cell size from the central region of cotyledons were determined using NIH IMAGE analysis software as described (Ohto

et al., 2005). The area of the cotyledon was calculated from 50 mature embryos. The cell size in the middle of the cotyledon was also determined from 20 mature embryos by dividing 130 μm^2 image area by the number of cells. Data are presented as the average of two independent experiments.

Scanning Electron Microscopy

Mature embryos from the mutant and the wild type were released from the seed coats by applying gentle pressure and fixed in FAA at 4°C for 2 h. After fixation, the samples were dehydrated through an ethanol series (70, 85, 95, and 100%), each for 30 min. The embryos were then dried using the Autosamdri-814 Critical Point Dryer. The individual embryos were mounted on scanning electron microscopy stubs, sputter-coated with gold with a Fullam Sputter-coater, and examined under a Hitachi S3500N variable pressure scanning electron microscope at an accelerating voltage of 5 k.

Protein, Carbohydrate, and Fatty Acid Analysis

Total proteins were extracted from the same number of wild-type and mutant seeds as described (Heath et al., 1986). Protein content was determined using the Bio-Rad DC protein assay kit with BSA as standard. Total protein extracts from 200 seeds of the wild type and mutants was also fractionated on 12% SDS-PAGE and stained with Coomassie Brilliant Blue as described (Ohto et al., 2005).

To extract total fatty acids, 100 seeds from wild-type and mutant plants were homogenized in 500 μL 1 N HCl-methanol, and 200 mL hexane was added to each vial and heated for 2 h at 85°C (Larson and Graham, 2001). After heating, the solutions were cooled and 250 μL 0.9% KCl was added to partition the hexane phase that contained the fatty acid methyl esters. A 1-μL aliquot of the hexane solution was then analyzed by gas chromatography with flame ionization detection. Free fatty acid C21:0 (Sigma-Aldrich) was added as an internal control. Total fatty acid content was estimated by comparing the total fatty acid methyl ester peak area to that of the C21:0 internal standard.

One hundred seeds each from the wild type and the *shb1* mutant were also homogenized in 500 mL of 80% ethanol, and the extracts were incubated at 70°C for 90 min (Focks and Benning, 1998). Following centrifugation, the supernatant was saved and the pellet was extracted twice again with 500 μL of 80% ethanol. The combined supernatants were evaporated, and the residue was dissolved in 100 μL of deionized water and measured for reducing sugars by the Nelson-Somogyi assay (Nelson, 1944; Somogyi, 1952). The total sugar content was measured using the phenol sulfuric acid carbohydrate assay and interpreted against a 1-mg/mL glucose-generated standard curve (Dubois et al., 1956).

Developmental Alteration Analysis

To examine the developmental alterations of *shb1* mutants, wild-type and *shb1* mutant flowers were hand-pollinated, and the developing seeds were harvested at different days after pollination. The siliques were then cut into 2-mm-long fragments, fixed, and dehydrated as described above. The segments were next cleared in Hoyer's solution overnight and examined using an Olympus BX51 with differential interference contrast optics. Data after 10 DAP were not collected as siliques were mature and preparation of clear seeds at these late developmental stages becomes difficult. To investigate endosperm development, the siliques were fixed in FAA solution overnight at 4°C, dehydrated as described above, and embedded in EPON 812 (SERVA). Sections were stained with 0.1% (w/v) toluidine blue O in distilled water. Stained sections were photographed using a Cool Cam color CCD camera (Cool Camera) coupled to an Olympus BH-2 microscope.

Real-Time RT-PCR Analysis

For quantitative RT-PCR analysis, total RNAs were isolated from green siliques 4 to 5 d after hand-pollination (i.e., early to late heart stage) using the SV Total RNA Isolation Kit (Promega). SuperScript III reverse transcriptase (Invitrogen) was used to synthesize the first-strand cDNA with oligo(dT) primer and 1 μg of total RNA at 50°C for 1 h. Quantitative PCR was then performed with the Platinum SYBR Green qRT-PCR Kit (Invitrogen) on an Applied Biosystems 7500 Real-Time PCR machine. The thermal cycling program was 50°C for 10 min and 95°C for 10 min, followed by 40 cycles of 95°C for 30 s, 56°C for 30 s, 72°C for 1 min, and a one-cycle dissociation stage at 95°C for 15 s, 60°C for 1 min, and 95°C for 15 s. The primers used in quantitative RT-PCR were *MINI3*, 5′-TTTGATGATATTGCAACGGAA-3′ and 5′-GATCCTTTGTGTCTTGCTTGT-3′; *IKU2*, 5′-CGTGTGAGACAAGCGTTAGC-3′ and 5′-GAGGAGACTTGTCCGTGCAT-3′; *AP2*, 5′-ATTCGGCTAATTCGAAGCATAA-3′ and 5′-AGAGGAGGTTGGAAGCCATT-3′; *SHB1*, 5′-CAGGTTCAAGCACTGAGGAGT-3′ and 5′-TGCTTCCTCGGTTTAGAGTA-3′; *HSF15*, 5′-CAACCTCAAAACTTCCTTTC-3′ and 5′-TAATGATTTCCACAAGGTGA-3′; and *UBQ10*, 5′-AGGTACAGCGAGAGAAAGTAGCA-3′ and 5′-TAGGCATAGCGGCGAGGCGT-3′. Data were calculated from three biological replicates, and each biological replicate was examined in triplicate.

Reciprocal Crosses and Double Mutant Analysis

The reciprocal crosses between Ws and *shb1-D* and between Col and *shb1* were made with flowers at identical positions (11th to 14th flowers) on secondary inflorescences. Seed weight and seed number per silique were determined from four separate inflorescences per plant and from four to five plants in total. A series of double mutants of *shb1-D* with small seed size mutants *mini3-2* and *iku2-4* were made and PCR genotyped. Gene-specific primers for *MINI3* are 5′-TGTCGTTGCAATCTCTCCA-3′ and 5′-GATCCTTTGTGTCTTGCTTGT-3′. Gene-specific primers for *IKU2* are 5′-TCTTTTTAATGCCACTAGCTT-3′ and 5′-CGAACATTCCAAGAGACACA-3′. Gene-specific primers for *SHB1* are 5′-TAAGCAGCACGAGCTCAAAT-3′ and 5′-TGCTTCCTCGGTTTAGAGTA-3′. Gene-specific primers for *AP2* are 5′-TAGGTGGATTTGACACTGCT-3′ and 5′-AGAGGAGGTTGGAAGCCATT-3′. The T-DNA–specific primer for *mini3-2*, *iku2-4*, *shb1*, and *ap2* is 5′-GGAACCACCATCAAACAGGAT-3′. For *shb1-D* genotyping, gene-specific primers are 5′-GAAGATACGGGTTTTGCAT-3′ and 5′-GGGAAGCTTGGATGTCTTGAA-3′, and the T-DNA–specific primer is 5′-CATTTTATAATAACGCTGCGGACATCTAC-3′.

ProSHB1:GUS Construct and GUS Staining

A 2886-bp *SHB1* promoter region was amplified by PCR using forward primer 5′-CTAAGCTTCTTCGCGTTATATGACACAACG-3′ and reverse primer 5′-GCGTCGACTGAATCTTGGCCTCTCTCTGTC-3′, which contain a *Hin*dIII and a *Sal*I restriction site (underlined), respectively. The PCR fragment was digested with *Hin*dIII and *Sal*I and inserted in frame in front of the *GUS* gene in the pCAMBIA1391 plasmid. The constructs were transformed into Ws by the floral dip method using *Agrobacterium tumefaciens* GV3101 (Clough and Bent, 1998). Transgenic plants were selected on 25 mg/L of hygromycin B medium (Roche). GUS staining was performed using the method of Sieburth and Meyerowitz (1997). Briefly, tissue was gently fixed by incubation in 90% acetone on ice for 15 to 20 min and rinsed with buffer that contains 50 mM $NaPO_4$, pH 7.2, 0.5 mM $K_3Fe(CN)_6$, and 0.5 mM $K_4Fe(CN)_6$. Tissue was then transferred to staining solution that contains 50 mM $NaPO_4$, pH 7.2, 2 mM X-gluc (Sigma-Aldrich), 0.5 mM $K_3Fe(CN)_6$, and 0.5 mM $K_4Fe(CN)_6$, vacuum infiltrated for 10 min, and incubated at 37°C overnight. After staining, tissue was hydrated with 70% ethanol for 1 h and cleared in Hoyer's solution. Ovules were observed using an Olympus BX51 microscope with

differential interference contrast optics. Other tissues were photographed using a Cool Cam color CCD camera coupled to an Olympus BH-2 microscope.

In Situ Hybridization

Ws wild-type flowers were hand-pollinated, and the developing seeds were harvested at different days after pollination. The harvested siliques were fixed in FAA overnight at 4°C, embedded in paraplast (Sigma-Aldrich) after dehydration, and sectioned at 8 μm. A 379-bp fragment specific to the 5′ end of the *SHB1* gene was amplified with forward primer 5′-GAGGTTTGGGAAAGAGTTTGTGTC-3′ and reverse primer 5′-AGCTGTCTCCACTTTCAGCCTG-3′ and cloned into the pGEM-T easy vector. Antisense and sense RNA probes were synthesized in vitro with digoxigenin-UTP by SP6 and T7 RNA polymerases (Digoxigenin RNA labeling kit; Boehringer Mannheim). Sections were hybridized with 200 ng/mL probes at 42°C overnight in hybridization solution that contains 50% formamide. Hybridization signals were detected using antidigoxigenin antibody conjugated to alkaline phosphatase (DIG nucleic acid detection kit; Boehringer Mannheim). Photographs were taken using a Cool Cam color CCD camera coupled to an Olympus BH-2 microscope.

Anti-SHB1 Antiserum and ChIP Assays

A PCR-generated 2-kb SHB1 C-terminal fragment was subcloned into the *Eco*RI and *Sal*I sites of the pET-30a expression vector. Approximately 3 mg of SHB1 protein was purified using a His-tag affinity column (Novagen) and injected into rabbits for polyclonal antibody production (Cocalico Biologicals). The specificity of the antibody was verified using preimmunoserum and the fourth bleeding serum in protein gel blot analysis.

ChIP assays were performed as described (Bowler et al., 2004; Sawa et al., 2007) with the following minor modifications. Briefly, developing siliques were harvested 4 to 5 d after hand pollination (early to late heart stage) and fixed with 1% formaldehyde under vacuum. Chromatins were incubated with either anti-SHB1 antibody or anti-GFP antibody for 3 h at 4°C and then incubated with protein A/G agarose beads that had been preequilibrated with salmon sperm DNA for another 2 h at 4°C. Preimmune serum was used as the negative control. After washing twice with low salt buffer and high salt buffer that contains 0.05% SDS and 0.5% Triton X-100, the immunocomplexes were eluted from the agarose beads twice using freshly prepared elution buffer at 65°C (Bowler et al., 2004). DNA was purified by phenol/chloroform extraction and recovered by ethanol precipitation in the presence of glycogen (Sawa et al., 2007). The DNA pellet was resuspended in 150 μL of water, and 3-μL aliquots were used for quantitative PCR analysis. Quantitative PCR was performed as described for real-time PCR analysis. The fold enrichment of the specific chromatin fragment was normalized to the expression level of the *UBQ10* amplicon and calculated for each amplicon using the following equation: $2^{(Ct\ MINI3\text{-}M1\ MOCK\text{-}Ct\ MINI3\text{-}M1\ ChIP)}/2^{(Ct\ UBQ10\ MOCK\text{-}Ct\ UBQ10\ ChIP)}$. The primer pairs used in real-time PCR experiments were as follows: *MINI3/M1*, 5′-CTCATTTTTGACAAATCCTT-3′ and 5′-AACCGAAGTAGAAACCTAAA-3′; *MINI3/M2*, 5′-TTGTTTTCAATTTTTCACAT-3′ and 5′-AACAAACGGTTATTTTTCTT-3′; *MINI3/M3*, 5′-TGATGGTATAGTACCGTGATCG-3′ and 5′-TTGGTTGGACTGGTAGAGTCAG-3′; *IKU2/IK1*, 5′-TCTCCGGTCTCTCTTGATAA-3′ and 5′-GTAGGCGAAACAACATAAGG-3′; *IKU2/IK2*, 5′-CCTTATGTTGTTTCGCCTAC-3′ and 5′-TCTCTACGTCGGAAGGATTA-3′; *LEC2/L1*, 5′-CACAAAAGAAAACGAGTCAA-3′ and 5′-TATAAGGAAGAGAGCCAAGG-3′; *LEC2/L2*, 5′-CTAAGTTAGTCGTTTTTCCA-3′ and 5′-ACTCGATTTTCACAAAACTA-3′; *HSF15/H1*, 5′-AGATACAATGTTGTGGACTT-3′ and 5′-ATTTTGGATCAAAAGCACTC-3′; *HSF15/H2*, 5′-GAGTCTTTTGGGTCTTTAAT-3′ and 5′-CATCTTTTGGTAAACAATCT-3′; *UBQ10*, 5′-TCCAGGACAAGGAGGTATTCCTCCG-3′ and 5′-CCACCAAAGTTTTACATGAAACGAA-3′.

Accession Numbers

Sequence data from this article can be found in the Arabidopsis Genome Initiative database under the following accession numbers *UBQ10* (At4G05320), *SHB1* (At4G25350), *AP2* (At4G36920), *MINI3* (At1G55600), and *IKU2* (At3G19700).

Supplemental Data

The following materials are available in the online version of this article.

Supplemental Figure 1. Silique Number of Wild-Type and *shb1* Mutants and Seed Mass per Wild-Type and *shb1-D* Plant under Various Light Conditions.

Supplemental Figure 2. Adult Vegetative and Reproducing Wild-Type and *shb1* Mutant Plants.

Supplemental Figure 3. Protein Content on the Basis of Seed Mass and Fatty Acid Composition of Wild-Type and *shb1* Mutants.

Supplemental Figure 4. Reducing and Total Soluble Sugar Content of Wild-Type and *shb1* Mutants.

Supplemental Figure 5. Expression and ChIP Analysis of *SHF15* and *LEC2*.

ACKNOWLEDGMENTS

We thank David Marks and Changbin Chen for help and suggestions on microscopy experiments. We thank Gilbert Ahlstrand from the College of Biological Science imaging center for help with scanning electron microscopy. We appreciate the help from Tom Krick with fatty acid analysis in the Center for Mass Spectrometry and Proteomics. We also thank the Ohio State Stock Center for *Arabidopsis* T-DNA insertion collections and mutant seeds. This work was supported by a grant from the National Research Initiative of the USDA Cooperative State Research, Education, and Extension Service (2004-35304-14939 to M.N.) and by a grant from the program for Changjiang Scholars and Innovative Research Team in University (PCSIRT, IRT0635 to X.Z.).

Received December 7, 2008; revised December 7, 2008; accepted January 5, 2009; published January 13, 2009.

REFERENCES

Bowler, C., Benvenuto, G., Laflamme, P., Molino, D., Probst, A.V., Tariq, M., and Paszkowski, J. (2004). Chromatin techniques for plant cells. Plant J. **39:** 776–789.

Berger, F. (2003). Endosperm, the crossroad of seed development. Curr. Opin. Plant Biol. **6:** 42–50.

Boisnard-Lorig, C., Colon-Carmona, A., Bauch, M., Hodge, S., Doerner, P., Bancharel, E., Dumas, C., Haseloff, J., and Berger, F. (2001). Dynamic analyses of the expression of the histone:YFP fusion protein in Arabidopsis show that syncytial endosperm is divided in mitotic domains. Plant Cell **13:** 495–509.

Brink, R.A., and Cooper, D.C. (1947). The endosperm in seed development. Bot. Rev. **13:** 423–541.

Canales, C., Bhatt, A.M., Scott, R., and Dickinson, H. (2002). EXS, a putative LRR receptor kinase, regulates male germline cell number and tapetal identity and promotes seed development in Arabidopsis. Curr. Biol. **12:** 1718–1727.

Clough, S.J., and Bent, A.F. (1998). Floral dip: A simplified method for

Agrobacterium-mediated transformation of *Arabidopsis thaliana.* Plant J. **16:** 735–743.

Downey, R.K. (1983). High and low erucic acid rapeseed oils. In Biochemical Aspects of Crop Improvement, J. Kamer, F. Sauer, and W. Pigden, eds (New York: Academic Press), pp. 253–292.

Dubois, M., Gilles, K.A., Hamilyon, J.K., Rebers, P.A., and Smith, F. (1956). Colorimetric method for determination of sugars and related substances. Anal. Chem. **28:** 350–356.

Focks, N., and Benning, C. (1998). *wrinkled1*: A novel, low-seed-oil mutant of Arabidopsis with a deficiency in the seed-specific regulation of carbohydrate metabolism. Plant Physiol. **118:** 91–101.

Garcia, D., Fitz Gerald, J.N., and Berger, F. (2005). Maternal control of integument cell elongation and zygotic control of endosperm growth are coordinated to determine seed size in Arabidopsis. Plant Cell **17:** 52–60.

Garcia, D., Saingery, V., Chambrier, P., Mayer, U., Jurgens, G., and Berger, F. (2003). Arabidopsis *haiku* mutants reveal new controls of seed size by endosperm. Plant Physiol. **131:** 1661–1670.

Heath, J.D., Weldon, R., Monnot, C., and Meinke, D.W. (1986). Analysis of storage proteins in normal and aborted seeds from embryo-lethal mutants of *Arabidopsis thaliana*. Planta **169:** 304–312.

Hong, S.K., Kitano, H., Satoh, H., and Nagato, Y. (1996). How is embryo size genetically regulated in rice? Development **122:** 2051–2058.

Hutchison, C.E., Li, J., Argueso, C., Gonzalez, M., Lee, E., Lewis, M.W., Maxwell, B.B., Perdue, T.D., Schaller, G.E., Alonso, J.M., Ecker, J.R., and Kieber, J.J. (2006). The Arabidopsis histidine phosphotransfer proteins are redundant positive regulators of cytokinin signaling. Plant Cell **18:** 3073–3087.

James, D.W., and Dooner, H.K. (1990). Isolation of EMS-induced mutants in Arabidopsis altered in seed fatty-acid composition. Theor. Appl. Genet. **80:** 241–245.

Jofuku, K.D., Omidyar, P.K., Gee, Z., and Okamuro, J.K. (2005). Control of seed mass and seed yield by the floral homeotic gene APETALA2. Proc. Natl. Acad. Sci. USA **102:** 3117–3122.

Kang, I.H., Steffen, J.G., Portereiko, M.F., Lloyd, A., and Drews, G.N. (2008). The AGL62 MADS domain protein regulates cellularization during endosperm development in *Arabidopsis.* Plant Cell **20:** 635–647.

Kang, X., and Ni, M. (2006). *Arabidopsis* SHORT HYPOCOTYL UNDER BLUE1 contains SPX and EXS domains and acts in cryptochrome signaling. Plant Cell **18:** 921–934.

Larson, T.R., and Graham, I.A. (2001). A novel technique for the sensitive quantification of acyl CoA esters from plant tissues. Plant J. **25:** 115–125.

Luo, M., Dennis, E.S., Berger, F., Peacock, W.J., and Chaudhury, A. (2005). MINISEED3 (MINI3), a WRKY family gene, and HAIKU2 (IKU2), a leucine-rich repeat (LRR) KINASE gene, are regulators of seed size in Arabidopsis. Proc. Natl. Acad. Sci. USA **102:** 17531–17536.

Miller, M.E., and Chourey, P.S. (1992). The maize invertase-deficient miniature-1 seed mutation is associated with aberrant pedicel and endosperm development. Plant Cell **4:** 297–305.

Nelson, N. (1944). A photometric adaptation of the Somogyi method for the determination of glucose. J. Biol. Chem. **153:** 375–380.

Ohto, M., Fischer, R.L., Goldberg, R.B., Nakamura, K., and Harada, J.J. (2005). Control of seed mass by APETALA2. Proc. Natl. Acad. Sci. USA **102:** 3123–3128.

Olsen, O.A. (2001). Endosperm development: Cellularization and cell fate specification. Annu. Rev. Plant Physiol. Plant Mol. Biol. **52:** 233–267.

Otegui, M.S., Capp, R., and Staehelin, L.A. (2002). Developing seeds of Arabidopsis store different minerals in two types of vacuoles and in the endoplasmic reticulum. Plant Cell **14:** 1311–1327.

Pang, P.P., Pruitt, R.E., and Meyerowitz, E.M. (1988). Molecular cloning, genomic organization, expression and evolution of 12S seed storage protein genes of *Arabidopsis thaliana*. Plant Mol. Biol. **11:** 805–820.

Riefler, M., Novak, O., Strnad, M., and Schmülling, T. (2006). Arabidopsis cytokinin receptor mutants reveal functions in shoot growth, leaf senescence, seed size, germination, root development, and cytokinin metabolism. Plant Cell **18:** 40–54.

Sawa, M., Nusinow, D.A., Kay, S.A., and Imaizumi, T. (2007). FKF1 and GIGANTEA complex formation is required for day-length measurement in Arabidopsis. Science **318:** 261–265.

Schruff, M.C., Spielman, M., Tiwari, S., Adams, S., Fenby, N., and Scott, R.J. (2006). The AUXIN RESPONSE FACTOR 2 gene of Arabidopsis links auxin signalling, cell division, and the size of seeds and other organs. Development **133:** 251–261.

Schultz, P., and Jensen, W.A. (1971). *Capsella* embryogenesis: The chalazal proliferating tissue. J. Cell Sci. **8:** 201–227.

Scott, R.J., Spielman, M., Bailey, J., and Dickinson, H.G. (1998). Parent-of-origin effects on seed development in *Arabidopsis thaliana*. Development **125:** 3329–3341.

Sieburth, L.E., and Meyerowitz, E.M. (1997). Molecular dissection of the *AGAMOUS* control region shows that cis elements for spatial regulation are located intragenically. Plant Cell **9:** 355–365.

Somogyi, M. (1952). Notes on sugar determination. J. Biol. Chem. **195:** 19–23.

Spain, B.H., Koo, D., Ramakrishnan, M., Dzudzor, B., and Colicelli, J. (1995). Truncated forms of a novel yeast protein suppress the lethality of a G protein subunit deficiency by interacting with the subunit. J Biol. Chem. **270:** 25435–25444.

Sundaresan, V. (2005). Control of seed size in plants. Proc. Natl. Acad. Sci. USA **102:** 17887–17888.

Stone, S.L., Kwong, L.W., Yee, K.M., Pelletier, J., Lepiniec, L., Fischer, R.L., Goldberg, R.B., and Harada, J.J. (2001). *LEAFY COTYLEDON2* encodes a B3 domain transcription factor that induces embryo development. Proc. Natl. Acad. Sci. USA **98:** 11806–11810.

Taylor, D.C., Giblin, E.M., Reed, D.W., Hogge, L.R., Olson, D.J., and MacKenzie, S.L. (1995). Stereospecific analysis and mass-spectrometry of triacylglycerols from *Arabidopsis thaliana* (L) heynh Columbia seed. J. Am. Oil Chem. Soc. **72:** 305–308.

Wigge, P.A., Kim, M.C., Jaeger, K.E., Busch, W., Schmid, M., Lohmann, J.U., and Weigel, D. (2005). Integration of spatial and temporal information during floral induction in Arabidopsis. Science **309:** 1056–1059.

Winter, D., Vinegar, B., Nahal, H., Ammar, R., Wilson, G.V., and Provart, N.J. (2007). An electronic fluorescent pictograph browser for exploring and analyzing large-scale biological data sets. PLoS One **2:** e718.

Xiao, W., Brown, R.C., Lemmon, B.E., Harada, J.J., Goldberg, R.B., and Fischer, R.L. (2006). Regulation of seed size by hypomethylation of maternal and paternal genomes. Plant Physiol. **142:** 1160–1168.

Zhao, D.Z., Wang, G.F., Speal, B., and Ma, H. (2002). The excess microsporocytes1 gene encodes a putative leucine-rich repeat receptor protein kinase that controls somatic and reproductive cell fates in the Arabidopsis anther. Genes Dev. **16:** 2021–2031.